Chemical Engineering Journal 431 (2022) 133445

Contents lists available at ScienceDirect

Chemical Engineering Journal

journal homepage: www.elsevier.com/locate/cej

Antifouling superhydrophobic surfaces with bactericidal and SERS activity

Furkan Sahin [a], Nusret Celik [a,b], Ahmet Ceylan [c], Sami Pekdemir [a,d], Mahmut Ruzi [a,*], M. Serdar Onses [a,b,e,*]

[a] ERNAM – Erciyes University Nanotechnology Application and Research Center, Kayseri 38039, Turkey
[b] Department of Materials Science and Engineering, Erciyes University, Kayseri 38039, Turkey
[c] Faculty of Pharmacy, Erciyes University, Kayseri 38039, Turkey
[d] Department of Aeronautical Engineering, Faculty of Aeronautics and Astronautics, Kayseri 38039, Turkey
[e] UNAM–Institute of Materials Science and Nanotechnology, Bilkent University, Ankara 06800, Turkey

ARTICLE INFO

Keywords:
Superhydrophobic surfaces
Antibacterial
Antifouling
SERS
Food packaging

ABSTRACT

Fouling and contamination of surfaces are prevailing challenges humanities facing today in fields such as healthcare, hospitality, and food manufacturing. These challenges strongly motivate the development of multifunctional surfaces with antifouling and antimicrobial properties that are coupled with sensing capabilities. To address this challenge, we prepared a multifunctional superhydrophobic surface using eco-friendly materials: polydimethylsiloxane (PDMS) and carnauba wax. After deposition of a thin film of Ag, the surface gained surface-enhanced Raman scattering (SERS) activity and bactericidal property. The multifunctional superhydrophobic surface showed extreme liquid repellency towards water and common liquid food. The strong SERS activity enabled the detection of adulterant rhodamine B in a sausage down to a nanomolar level. Notably, the surface showed excellent bactericidal activity towards two common bacteria, *E. coli,* and S. aureus, significantly reducing their adhesion and killing. Additionally, the surface showed anti-fouling behavior against common liquid food, and even towards sticky foods such as yogurt, honey, and pomegranate sauce, reducing residual food by >97 %. Furthermore, the superhydrophobic surface showed excellent chemical stability in dynamic and static flow conditions and leaching of Ag in neutral and basic solutions was minimal.

1. Introduction

Fouling and contamination of surfaces is a significant challenge in everyday life and industry. Fouling of watercraft leads to corrosion and increased hydrodynamic drag. Fouling, particularly by microorganisms, can be deadly in the food and healthcare industry. Furthermore, the issue leads to associated economic burdens and social challenges. For example, methicillin-resistant Staphylococcus aureus (S. aureus) and third-generation cephalosporin-resistant Escherichia coli (E. coli) caused bloodstream infection in Europe in 2007 alone resulted in an estimated 8000 deaths and extra costs worth 62 million euros [1]. As a result, various methods have been developed to tackle contamination and fouling. A traditional approach is regular cleaning and disinfection of surfaces [2,3]. However, increasing costs and concerns about safety, pollution, and antimicrobial resistance is encouraging researchers to develop alternative approaches. One such method is the modification of surfaces to mitigate the adhesion of contaminants and microorganisms [4–6]. In this regard, imparting superhydrophobicity is emerging as an attractive approach [7–10].

Superhydrophobic surfaces possess rough micro/nanoscale morphology and low surface energy. On such surfaces, liquids sit atop the air pockets entrapped between the asperities of the protrusions, i.e., in a Cassie-Baxter state [11,12]. Here, liquid droplets display large contact angles and easily roll-off, thanks to reduced adhesion force [13]. Those features of superhydrophobic surface include self-cleaning [14,15], anti-corrosion [16,17], anti-biofouling [18–20], and drag reduction [21,22]. However, superhydrophobicity alone is not enough to completely resolve contamination and fouling, especially if the fouling agent is living microorganisms [18,23]. Notably, superhydrophobicity can even worsen contamination and microbial growth if the culprit fits into the cavities, displacing air pockets upon transition into Wenzel state [12,18,24–26]. A remedy is the addition of bactericidal agents where the superhydrophobicity reduces the chance of adhesion and the antibacterial property inactivates the microorganism. However, surging antimicrobial resistance invalidates the usage of conventional bactericidal agents [6].

* Corresponding authors at: ERNAM – Erciyes University Nanotechnology Application and Research Center, Kayseri 38039, Turkey (M. Serdar Onses).
E-mail addresses: mruzi17@gmail.com (M. Ruzi), onses@erciyes.edu.tr (M.S. Onses).

https://doi.org/10.1016/j.cej.2021.133445
Received 23 August 2021; Received in revised form 17 October 2021; Accepted 1 November 2021
Available online 6 November 2021

Metals, such as Ag and Cu, have been used for centuries to deal with microbial, and have recently re-emerged as efficient wide spectrum antibacterial agents [27–29]. Additionally, one advantage of these metals over other antibacterial agents is the possibility of added surface-enhanced Raman scattering (SERS) activity [30]. Here, nanoscale architectures prepared from these metals enable enormous enhancement of Raman signals, due to the coupling of surface plasmon and electromagnetic light field [31]. Furthermore, superhydrophobic surfaces can be used to enhance the local concentration of analytes and thus improve the detection limit in SERS analysis, due to the large contact angle of aqueous droplets on superhydrophobic surfaces and minimal liquid–solid contact area wherein the dried analytes will be concentrated [32]. Therefore, it is possible to fabricate an antifouling, antimicrobial, and SERS active multifunctional superhydrophobic surface via the incorporation of metals like Ag.

The objective of this study is the preparation of a multifunctional superhydrophobic surface, which has great application potential in fields ranging from biomedical engineering to the food industry. In particular, an area for immediate application is for food packaging to extend shelf life, detect chemicals, and reduce food waste [3]. The incorporation of antimicrobials into superhydrophobic packaging materials decreases food spoilage, cross-contamination, and food-borne illness [19,33]. The SERS activity enables the detection of harmful adulterants [34,35]. On the other hand, the superhydrophobicity alone endows packaging material self-cleaning property, which is beneficial for cleaning and reducing residual food waste [36–41]. The latter aspect is significant, considering around 30 % of all produced food got wasted globally against the backdrop of millions in the underdeveloped world without enough to eat [42].

In this study, we present a novel multifunctional surface that incorporates superhydrophobicity, SERS activity, and antibacterial property in one platform. Here, the surface is fabricated via transferring the surface structure of the typical print paper to polydimethylsiloxane (PDMS), followed by spray-coating of carnauba wax dispersion and thermal vapor deposition of Ag. Besides multifunctionality, another advantage of the proposed fabrication approach is that it does not contain any toxic and unsustainable chemicals such as fluorocarbons and harsh organic solvents. The coating is composed of only PDMS and carnauba wax, which are highly eco-friendly and even used as food and medicine ingredients [43,44]. Moreover, the addition of small amounts of Ag does not compromise the advantages, since the usage of Ag for antiseptic purposes is widespread and can be found in some commercial products [3,45]. We particularly demonstrate the promise of the proposed multifunctional superhydrophobic surfaces in food packaging applications based on the self-cleaning characteristic against viscous sticky food, chemical durability, and minimal material leaching properties.

2. Materials and methods

2.1. Materials

PDMS (Sylgard 184) was bought from Dow Corning. Print paper, which is used as a mold to transfer its structure, was bought from a local store. Carnauba wax (No. 1 yellow) was bought from Sigma-Aldrich and ethanol (96%) was bought from Alkokim. Silicon wafer was purchased from Wafer World Inc.

2.2. Methods

2.2.1. Fabrication

The substrate was prepared in a three-step process. First, the surface structure of print paper was transferred to PDMS via replica molding, resulting in a structured PDMS film that features micro-channels, complementary to the surface structure of A4 paper [46,47]. This substrate is called PDMS-Paper. As a control sample, a thin PDMS film was also prepared via casting. For spray coating, a carnauba wax dispersion in ethanol was prepared by dissolving 0.4 g of carnauba wax in boiling ethanol (20 mL), followed by stirring for 30 min. Then, the carnauba wax dispersion was spray-coated from 20 cm. After complete evaporation of the solvent, the wax-coated PDMS-Paper surface was abraded against an aluminium foil for 30 cm under a load of 200 g. Afterwards, the substrate was coated with Ag using the thermal vapor deposition method (see pictures of coated samples in the supporting materials Fig. S1). Specifically, the structured PDMS coated with carnauba wax was fixed to the top of a vacuum chamber using double-sided tape and was rotated at 10 rpm while evaporated Ag was deposited on the sample surface. Ag pellet (purity, 99.99%) was used as the metal source. Before thermal vapor deposition, the vacuum chamber (NVTH-350, NanoVak) was evacuated to 2×10^{-8} Torr and maintained at 2.3×10^{-6} Torr during the deposition. The deposition rate of Ag was 0.4 Å/s as monitored using a quartz crsytal microbalance (QCM) via a thin film deposition monitor (SQM-160, Inficon). Note that the reported thickness values are based on the readings obtained via QCM. The amount of deposited Ag could be controlled by adjusting the deposition time. It should be noted that the deposited Ag is typically not a continuous film but instead forms nanoislands and grains [48,49].

2.2.2. Characterization of surface structure and wetting property

Morphology of the surfaces was characterized using a scanning electron microscope (SEM, Zeiss EVO LS10) at 25 kV and elemental analysis and mapping were performed using an energy dispersive detector (XFlash 6110, Bruker) attached to the SEM instrument. Samples were sputter-coated with a thin layer of gold before surface analysis. Contact angle (CA) and sliding angle (SA) were measured via an optical tensiometer (Atension, theta Lite) using liquids with volumes of 10 μL and 5 μL, respectively. The CA and SA on each surface were measured on at least three different points and the average values were reported, which are typically accurate to 2°.

2.2.3. SERS activity

For SERS measurements, a confocal Raman Microscope (Alpha 300 M+, WITec, Germany) with a laser excitation wavelength of 532 nm was used. The SERS spectra were obtained using a 100 × objective for an integration time of one second. The focused laser power at the sample surface is 100 μW. To evaluate the SERS activity of various surfaces coated with Ag (Fig. 2b and 2d), a 10 μL solution of rhodamine 6G (Sigma-Aldrich) in water was spotted on each surface and left to dry at room temperature, followed by taking the spectra. To calculate the limit of detection of rhodamine 6G, its solutions in water with concentrations of 100 fM, 1 pM, 10 pM, 100 pM, 1 nM, and 10 nM were prepared and a 10 μL of each solution was spotted on the superhydrophobic Ag@Wax@PDMS-Paper surface and allowed to dry at room temperature. SERS spectra were taken afterward following the same protocol as stated at the beginning of this paragraph. The limit of detection for rhodamine 6G was calculated using the intensity of the peak at 611 cm^{-1}. The analytical enhancement factor (AEF) was calculated using the formula below:

$$AEF = \frac{I_{sample}/C_{sample}}{I_{reference}/C_{reference}}$$

Here, I_{sample} and $I_{reference}$ are the signal intensity of rhodamine 6G peak at 611 cm^{-1} on the superhydrophobic Ag@Wax@PDMS-Paper surface and on the reference Si wafer surface, respectively. C_{sample} and $C_{reference}$ are the concentration of the rhodamine 6G spotted on the corresponding surfaces.

To evaluate the potential of the superhydrophobic Ag@Wax@PDMS-Paper surface to be used as a SERS active substrate to detect chemicals in food, we characterized rhodamine B (≥98%, Acros Organics) added as an adulterant in a sausage (bought from a local store) [34,50]. Due to the lack of reference samples, sausage samples were pretreated with

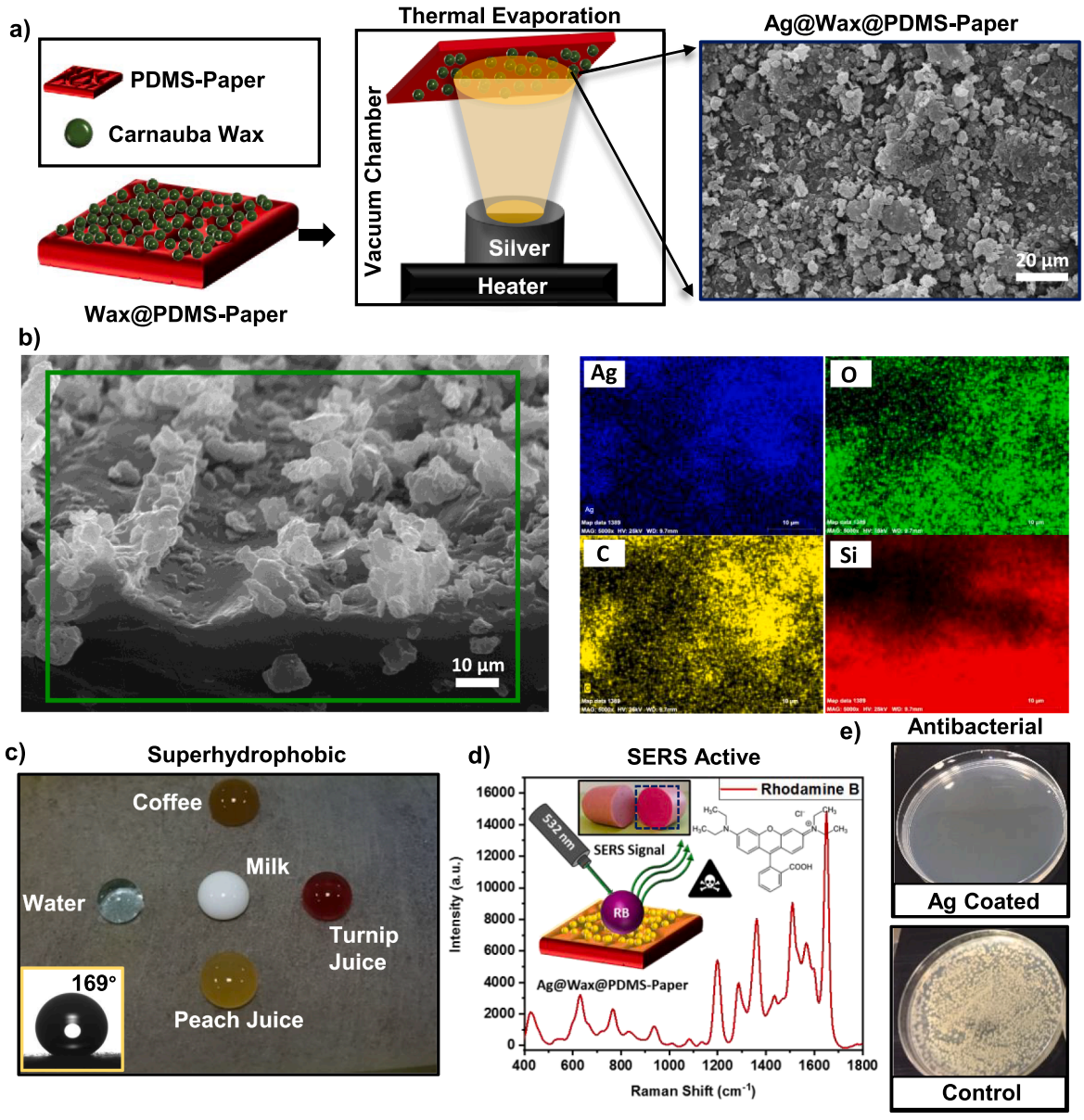

Fig. 1. Illustration and demonstration of the multifunctionality of the superhydrophobic Ag@Wax@PDMS-Paper surface. a) Illustration of the fabrication process and the SEM image of the fabricated superhydrophobic surface. b) SEM image (tilted 55°) and EDX elemental mapping of various elements. c) Photograph of various liquids on the fabricated superhydrophobic surface, where water (dyed blue) and other common liquid foods bead up and exhibit large CA. d) Demonstration of SERS activity of the surface, showing detection of rhodamine B adulterant in a sausage. e) Demonstration of antibacterial activity against *E. coli*. Shown in the pictures are *E. coli* colonies grown on the agar plate. The *E. coli* inoculants were transferred from the superhydrophobic Ag@Wax@PDMS-Paper (top) sample immersed in nutrient broth and the control sample (bottom, Wax@PDMS-Paper) immersed in nutrient broth.

rhodamine B, following a similar procedure to other studies [34,35]. For that purpose, we intentionally spiked sausages with known concentrations of rhodamine B, followed by dissolving the spiked sausage and

taking SERS spectra. Specifically, a 1 mM rhodamine B stock solution in water was prepared and diluted to obtain solutions with rhodamine B concentrations of 100 µM, 1 µM, 100 nM, and 1 nM. Then, 2 mL solution from each concentration was transferred to 15 mL conical bottom centrifuge tubes, followed by adding 0.5 g freshly cut sausages into each tube. The mixture of sausages and rhodamine B was sonicated at 40 kHz (Wiseclean) for 30 min to allow the sausage to adsorb rhodamine B, and then the sausage was taken out and left to dry at room temperature. Here, the sausage pieces spiked with rhodamine B represent adulterated sausages. The adulterant sausage pieces were then immersed into a 2 mL water: methanol mixture (10:1 v/v) and sonicated for 30 min, followed by vortexing for 2 min to separate solid pieces from the solution. Afterward, 10 µL of the solution was spotted on the superhydrophobic Ag@Wax@PDMS-Paper surface and the SERS spectrum was obtained.

2.2.4. *Anti-adhesion and bactericidal activity*

The anti-adhesion and bactericidal activity of the surfaces against the gram-negative *E.coli* (ATCC25922) and gram-positive *S.aureus* (ATCT25923) bacteria were evaluated according to the method of J. Haldar *et al.* with some modifications [51]. The bacteria strains were grown on Mueller-Hinton agar plates (Merck) and incubated at 37 °C for 24 h in an incubator (Innova 42, New Brunswick Scientific). A single colony was taken from the overnight culture and inoculated onto Mueller-Hinton broth medium. The inoculum strains were adjusted to the 0.5 McFarland standard turbidity (approximately 1.5 x10^8 CFU/mL)

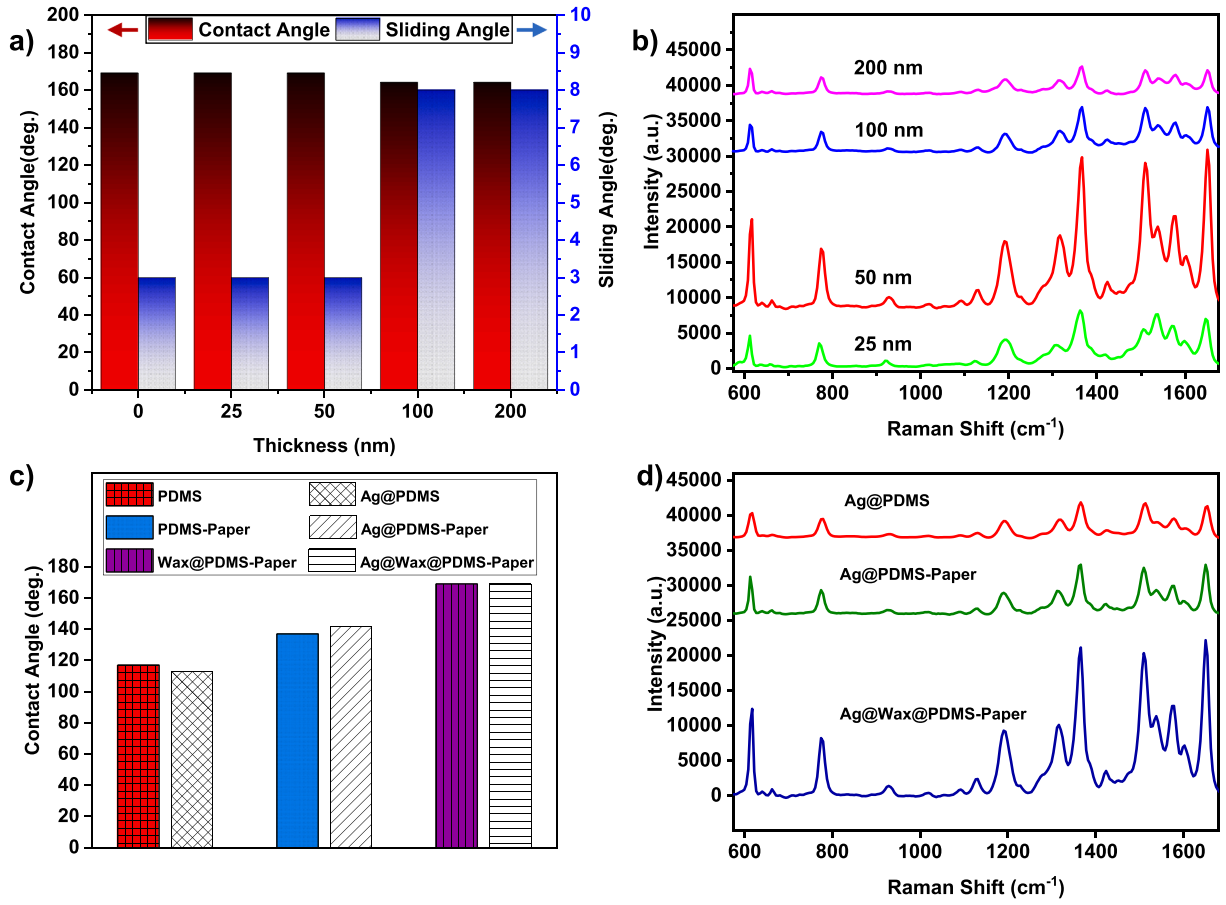

Fig. 2. Impact of vapor-deposited Ag on the wetting property and SERS activity. Shown are the effect of Ag thickness on the a) water CA and SA, and b) SERS signal of the probe molecule rhodamine 6G on the Wax@PDMS-Paper surface. c) The water CA and SA on various surfaces before and after coated with 50 nm of Ag. d) The SERS signal of rhodamine 6G on various surfaces coated with 50 nm of Ag. Note: the concentration of rhodamine 6G in b) and d) is 1×10^{-8} M.

using a densitometer (Den-1, Biosan).

For the anti-adhesion test, various samples (1.5 cm × 1.5 cm) were immersed in the bacteria culture and incubated at 37 °C with shaking at 150 rpm for 36 h. Afterward, the samples were retrieved and gently rinsed with deionized water to remove loosely attached bacteria. The number of attached bacteria was characterized via SEM imaging to infer the anti-adhesion ability of various surfaces against the two strains of bacteria.

Bactericidal tests were performed following the procedure illustrated in the supporting material (Fig. S2). Specifically, a 100 μL of bacteria culture was sprayed onto each sample surface using a chromatography sprayer, followed by covering with solid Mueller-Hilton agar medium and incubating at 37 °C for 24 h. Then, the agar medium was removed, and the samples were immersed into a Mueller-Hilton broth medium at 37 °C for 6 h to allow live bacteria to swim into the nutrient medium. Afterward, a 1.5 mL of nutrient was retrieved using a micropipette (Nichipet Ex-II, Nichiryo) and transferred to a quartz cuvette (path-length = 10 mm), followed by measuring the absorbance value at 600 nm using a UV–Vis spectrometer (Lambda 25, PerkinElmer). In the UV–Vis measurements, the absorbance of nutrients (1.5 mL) without bacteria was used as the reference. Besides absorbance measurements, the bactericidal efficacy of samples was characterized using the spread plate method where 100 μL of bacterium nutrient solutions were extracted using micropipettes and inoculated onto agar plates. The amount of CFU was visually inspected after incubating at 37 °C for 24 h. All bacterial studies were performed in Class II Microbiological Safety Cabinets (Faster SafeFAST Classic).

2.2.5. *Evaluation of anti-fouling and reduction of residual food*

For self-cleaning tests, liquid foods (bought from a local store) were poured onto tilted surfaces and the degree of stuck food was visually inspected. To evaluate the degree of residual food, we evaluated residual food left on the superhydrophobic surface, and control samples (glass, PET, aluminum) with a slight modification of a previously reported method [52]. Here, the substrates were cut into pieces of 1 cm × 1 cm, and the weight of each was measured. Then, the substrates were placed horizontally on a flat desk, followed by placing ~ 1 g each of honey, yogurt, pomegranate syrup, and milk and holding for 1 min. Consequently, the substrates were turned up and held vertically for 1 min to allow the food content to roll off, followed by measuring the weight immediately. Then, the weight increase on each substrate was calculated (sample weight with residual food – initial sample weight) and the percentage of residual food left on each substrate to initial food weight was reported as a residual percentage.

2.2.6. *Evaluation of durability*

2.2.6.1. Ag leaching tests. The stability of the Ag coated surfaces was evaluated by immersing them in solutions with pH of 1, 7, and 13 and then measuring Ag concentration after 1 day, 7 days, and 21 days. Solutions with pH = 1 and pH = 13 were prepared using aqueous HCl and NaOH, respectively. Deionized water was used as the neutral solution (pH = 7). The pH values of the solutions were measured using a laboratory pH meter (InoLab pH7110). For the leaching test, Ag coated substrates (1.5 cm × 1.5 cm) were immersed into 40 mL solutions in a beaker and kept in a lab for the duration of the test. A solution of liquid with a volume of 2 mL was withdrawn using a pipette after day 1, day 7,

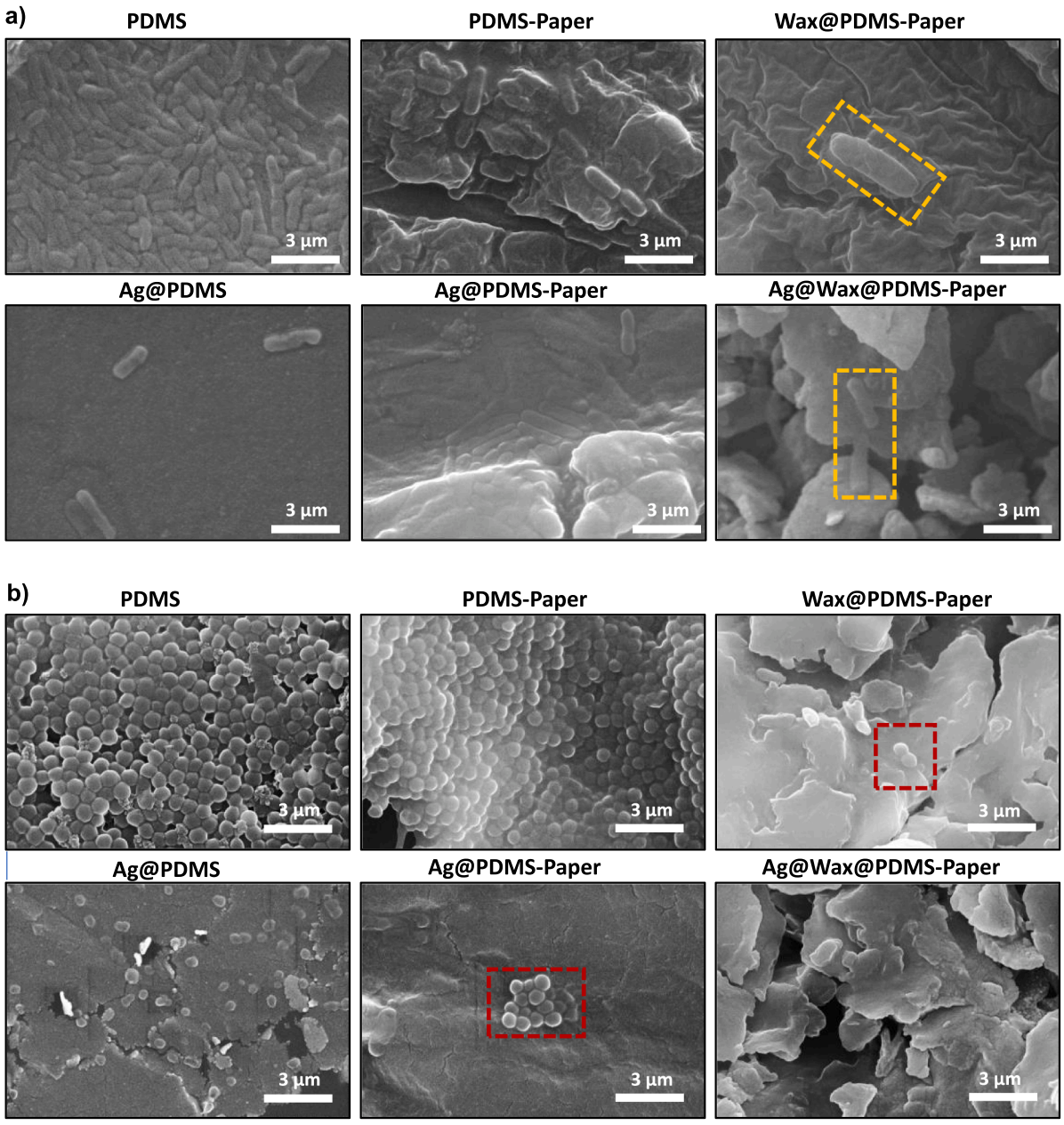

Fig. 3. Characterization of surface-adhered bacteria. Shown are SEM images of a) *E. coli* and b) S. aureus bacteria attached to various surfaces before and after being coated with 50 nm of Ag. For characterization, various surfaces are immersed into bacterium culture (~1.5 × 10^8 CFU/mL) and incubated at 37 °C with shaking at 150 rpm for 36 h. Afterward, the samples were retrieved and gently rinsed with deionized water. The SEM images were taken after the samples were dried. Some bacteria colonies are highlighted to help with discerning.

and day 21, and the Ag concentration was measured using inductively coupled plasma mass spectroscopy (ICP-MS, model 7500a, Agilent). The ICP-MS operating parameters were periodically optimized using a standard solution (in HNO_3) containing 200 ppb Li, Yb, and Cs. The calibration of ICP-MS was done using an internal standard solution containing 200 ppb of Be, Sc, Rh, Bi.

2.2.6.2. Mechanical durability tests. Various tests were conducted to evaluate the thermal and mechanical durability of the superhydrophobic surface. Thermal stability of the Ag@Wax@PDMS-Paper surface was evaluated by heating the sample on a hot plate at a specified temperature for 3 min and waited for it to cool down, followed by measuring the water CA and SA values. Mechanical durability of the surface was evaluated using three different methods under dynamic conditions. A water spray impact test was performed by spraying water (7.41 kPa) on the sample surface from 7.5 cm using a high-pressure spray gun. Underwater stability was evaluated by submerging the sample in water, and in acidic (pH = 1) and basic (pH = 13) solutions, followed by mechanically stirring at 50 rpm for 24 h. After that, the samples were retrieved, followed by blow-drying with nitrogen gas and measuring water CA and SA. The third test was performed to evaluate the stability of the superhydrophobic surface against the relative liquid motion. Specifically, the superhydrophobic surface was vertically submerged and retrieved at a speed of 1 cm/s from water, milk, and yogurt, and counted as one cycle. The water CA and SA values on the sample were measured after 100 cycles of the test.

3. Results and discussion

The multifunctional superhydrophobic surface is fabricated in a

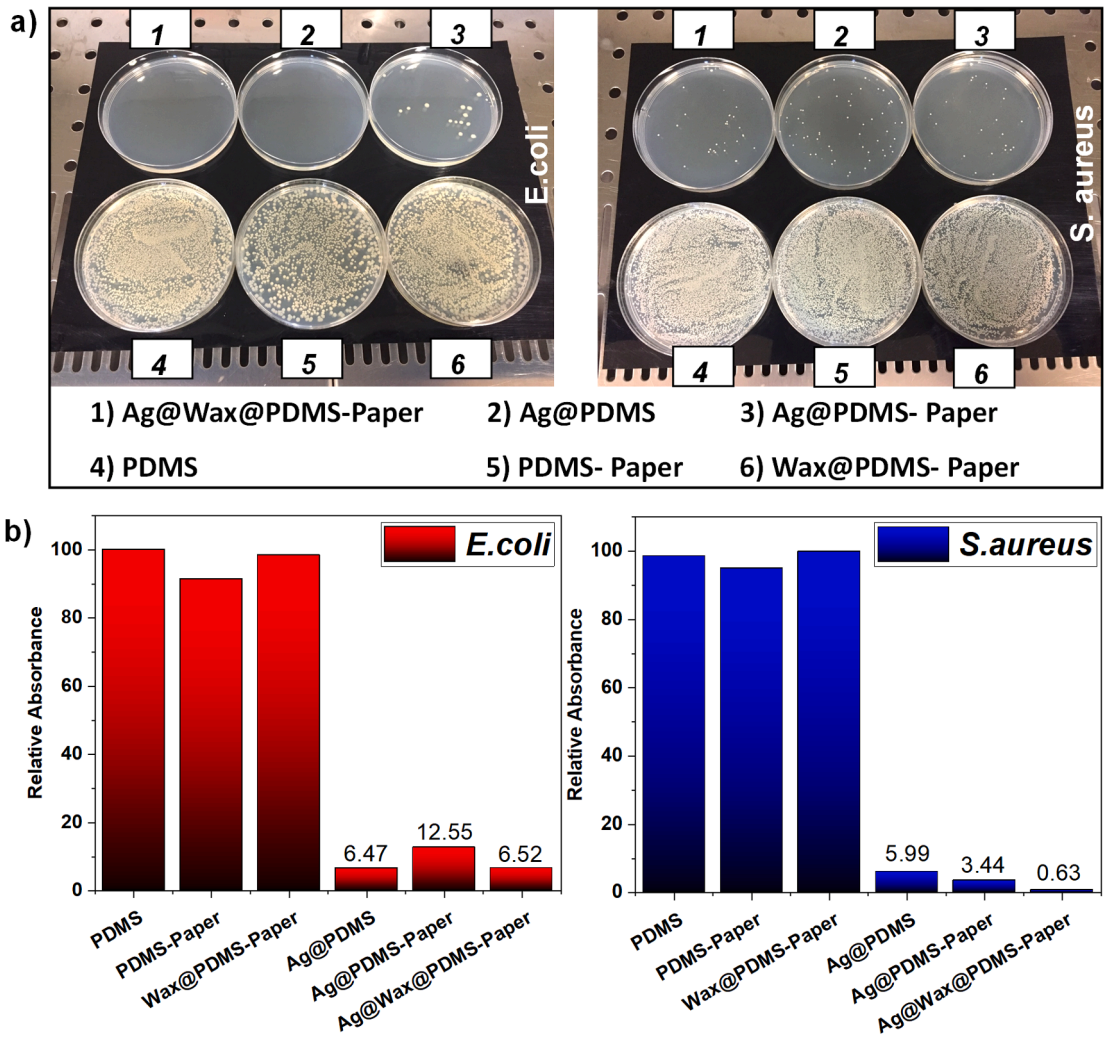

Fig. 4. Antibacterial activity of various surfaces. Shown are a) transferred bacteria grown on the Agar plate (left: *E. coli*, right: *S. aureus*) and (b) relative absorbance (at 600 nm) of the transferred bacterium solution. Here, the bacteria strains were overnight incubated on various sample surfaces, then immersed into a nutrient broth to allow live bacteria to swim into the broth and proliferate. Then, 100 μL of bacterium suspension was withdrawn and inoculated on the Agar plate (a). For quantitative measurement, 1.5 mL of bacterium suspension was withdrawn and absorbance value at 600 nm was recorded (b). The relative values were calculated with respect to the absorbance value (0.5552) of the *E. coli* bacterium suspension transferred from PDMS immersed cultured broth medium and *S. aureus* bacterium suspension transferred from the Wax@PDMS-Paper immersed in cultured medium (absorbance = 11.75).

three-step process. First, the fibrous surface structure of a piece of print paper was transferred to PDMS via replica molding, following the same procedures as described in our previous studies [46,47]. At the end of this step, a rough PDMS film with microchannels (negative replica of the paper surface) was obtained (PDMS-Paper). In the second step, the dispersion of carnauba wax in ethanol was spray-coated on the structured-PDMS surface to introduce nanoscale roughness [53]. In the last step, a thin layer (50 nm, 1250 s deposition time) of Ag was deposited on the surface of wax-coated rough PDMS surface (Wax@PDMS-Paper) by thermal evaporation of Ag, as illustrated in Fig. 1a. Since the amount of deposited Ag was only 50 nm, the Ag@Wax@PDMS-Paper surface exhibited similar surface morphology to the superhydrophobic Wax@PDMS-Paper surface (Fig. 1.a SEM image). The fabricated surface looks gray with some shine (supporting Fig. S1), due to high refractive indices of Ag and strong roughness-induced light scattering. The deposition of Ag was confirmed via EDX mapping (Fig. 1b) and EDX elemental analysis (supporting Fig. S3). A detailed inspection of EDX mapping reveals reduced deposition of Ag at the bottom of microchannels, which is probably due to the shadowing of the asperities where most Ag was deposited (Fig. 1b). On the macroscale (supporting Fig. S3), the deposition of carnauba wax dispersion, as well as the thermal deposition of Ag, was homogenous, and the coated sample contains 2.02 % Ag (atom %).

The multifunctional Ag@Wax@PDMS-Paper surface is extremely repellent to water and other liquids (Fig. 1c) where the droplets bead up, exhibiting a water CA of 169°. Furthermore, due to the presence of Ag, the superhydrophobic surface also shows strong SERS activity where even a small amount (nM level) of rhodamine B adulterant in a sausage can be detected (Fig. 1d). Moreover, the superhydrophobic surface also shows antibacterial activity against *E. coli* (Fig. 1e) and S. aureus. In summary, the fabricated Ag@Wax@PDMS-Paper surface is superhydrophobic, SERS active, and antibacterial. These characteristics are appealing for a range of applications, including smart food packaging.

The deposition of a thin layer of Ag imparted SERS activity to the superhydrophobic surface. To investigate the effect of the thickness of Ag on the surface wetting properties and SERS activity, samples with various Ag thicknesses (25 nm, 50 nm, 100 nm, and 200 nm) were prepared (Fig. 2). Up to Ag thickness of 50 nm, both the water CA (169°) and SA (3°) values on the Ag@Wax@PDMS-Paper surface remain the same (Fig. 2a). When 100 nm of Ag was deposited, the water CA decreased to 164° while the SA increased to 8°. Further increase of Ag thickness to 200 nm does not alter the wetting properties significantly. It

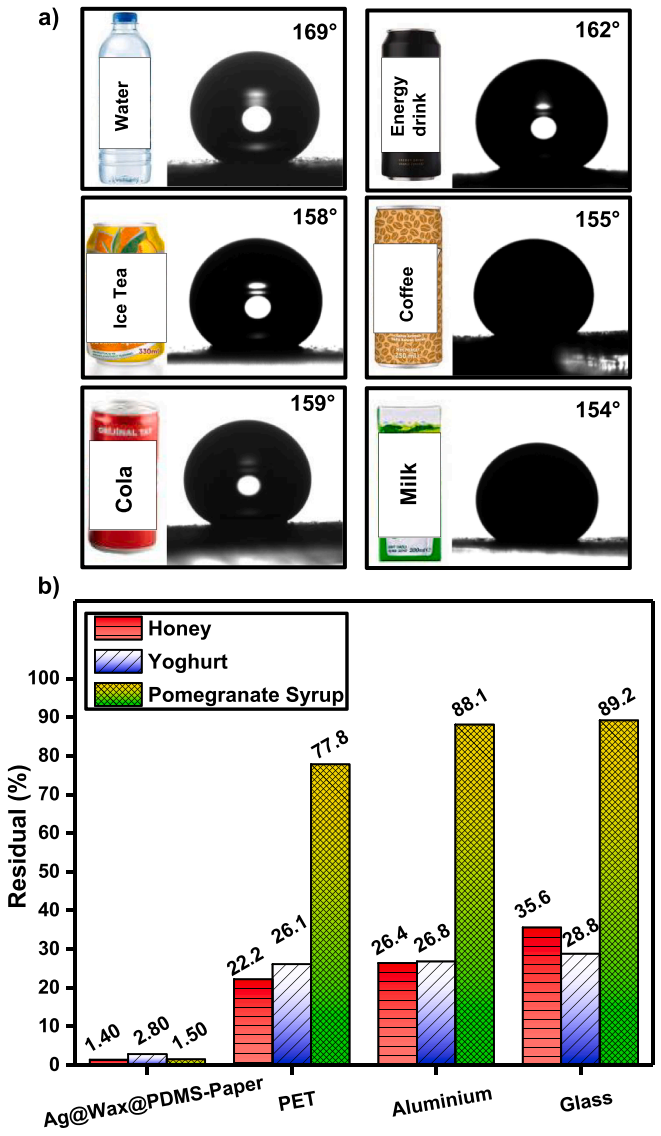

Fig. 5. Wetting property and stickiness characterization of various liquid food on the superhydrophobic Ag@Wax@PDMS-Paper surface. a) CA of various liquid food on the superhydrophobic surface. The CA was measured by placing a 10 μL droplet of each liquid. b) Food residual (%) stuck on the superhydrophobic surface, calculated as the percentage of liquid left (weight) after holding the superhydrophobic surface upright. For comparison, the residual percentage was also evaluated for food packaging materials PET, aluminum, and glass.

should be noted that the thermal vapor-deposited Ag typically does not form continuous thin film unless an adhesive layer such as germanium were used, and the deposited Ag forms large grains and nanoislands [48,49]. The observed wetting behavior of the Ag deposited surface is consistent with a previous study where the water CA initially increases as the Ag deposition time increases, then start to decrease upon further deposition of Ag [49]. It was reported that the trend can be explained as the change of surface roughness with the help of the Cassie-Baxter equation. Similarly, the surface deposited with 100 nm of Ag looks smoother than the sample with 50 nm Ag (supporting materials Fig.S4). It was expected that as the amount of deposited Ag increases the grain size of Ag will increase. However, due to the roughness of the underlying Wax@PDMS-Paper, the deposited Ag may fill in the cavities and, therefore, decrease the roughness. The surface morphology of the samples supports this hypothesis (Fig.S4). Besides wetting property, the amount of deposited Ag impacts the SERS activity (Fig. 2b). It was found that the SERS intensity (rhodamine 6G as the probe molecule) increases up to Ag thickness of 50 nm and peaks there, and then starts to decrease as Ag thickness increased up to 200 nm. The trend of SERS intensity change as a function of deposited Ag thickness implies an initial increase in the number of plasmonic nanogaps, which then start to decrease as further deposited Ag fills in the gaps [48]. We selected Ag thickness of 50 nm based on the results on the effect of the thickness of Ag on the wetting property and SERS activity. Hence, all Ag coated samples mentioned in the study refer to Ag thickness of 50 nm, unless stated otherwise.

To further investigate the impact of the substrate on the wetting property and SERS activity, we prepared a series of surfaces (PDMS, PDMS-Paper, and Wax@PDMS-Paper; see supporting materials Fig.S5 for SEM images) and measured the water CA and SA and recorded the SERS spectra of a probe molecule (rhodamine 6G) on these surfaces before and after coated with 50 nm of Ag. As shown in Fig. 2c, the deposition of Ag does not significantly affect the wetting property of all three surfaces. After deposition of Ag, all three surfaces show some SERS activity, the magnitude of which forms a positive correlation with surface hydrophobicity (Fig. 2d). For example, the intensity of the peak at 1361 cm^{-1} (rhodamine 6G) on the superhydrophobic Wax@PDMS-Paper surface (CA = 169°) is almost 4 times of that on the Ag@PDMS-Paper surface (CA = 142°, SA > 10°) which itself is ~ 1.5 times that of the Ag@PDMS (CA = 113°) film (supporting Fig. S6). The observed high SERS activity on the superhydrophobic surface is consistent with previous studies and can be traced to the 'concentrating' effect of superhydrophobic surfaces [30,54]. Specifically, on a superhydrophobic surface, a droplet has minimal contact area and upon evaporation of the solvent (water), the solute will be deposited only on that area, thus increasing the local concentration of the probe molecule.

As discussed in the previous section, the thickness of the deposited Ag was chosen as 50 nm (1250 s of deposition time) for simultaneous achievement of superhydrophobicity and high SERS activity. Furthermore, the superhydrophobic SERS platform shows very good spot-to-spot and sample-to-sample reproducibility (relative standard deviation ~ 10%, supporting Fig. S7) compared to state-of-the-art SERS substrates [31,55]. On this superhydrophobic SERS platform, the analytic enhancement factor is 5.26×10^8 and 100 fM levels of rhodamine 6G can be detected (supporting materials Fig. S8). Taking advantage of the high SERS activity, we studied the detection of adulterant rhodamine B in sausages. This study was motivated by the findings that some manufacturers illegally add rhodamine B to sausages to enhance color and that rhodamine B is a toxic chemical [34,35,56]. Therefore, there is a need to detect even the minute amounts of the adulterant molecule for food regulation and public health purposes. We found that adulterant rhodamine B down to 1 nM concentrations can be successfully detected in sausages (supporting materials Fig. S9). The detection level is on par with the best reported values and is two orders of magnitude better than the detection limit reported in a recent study [35].

Due to low surface energy and trapped air pockets, superhydrophobic surfaces reduce the chance of bacterial adhesion [57]. We tested the anti-adhesion ability of various surfaces to prevent the attachment of bacteria. The results are shown in Fig. 3 (also see supporting Fig. S10). Here, the SEM images are taken after gently rinsing the incubated sample surfaces with water. Therefore, only firmly attached bacteria would be left on the surface. Before being coated with Ag, the number of attached bacteria on the superhydrophobic surface is minimal (Fig. 3a and b, top rows). As a matter of fact, we had to search for bacteria for the SEM imaging. On the other hand, there are multiple colonies on the other two surfaces (PDMS and PDMS-Paper) with an attachment density that depends on the bacteria type. For *E. coli* (Fig. 3a, top row), the number of attached bacteria on the PDMS (CA = 113°) is larger than that on the PDMS-Paper surface (CA = 142°), which itself is much larger than that on the superhydrophobic Wax@PDMS-Paper surface (CA = 165°). The trend is consistent with previous studies where it is found that the more hydrophobic a surface is the less

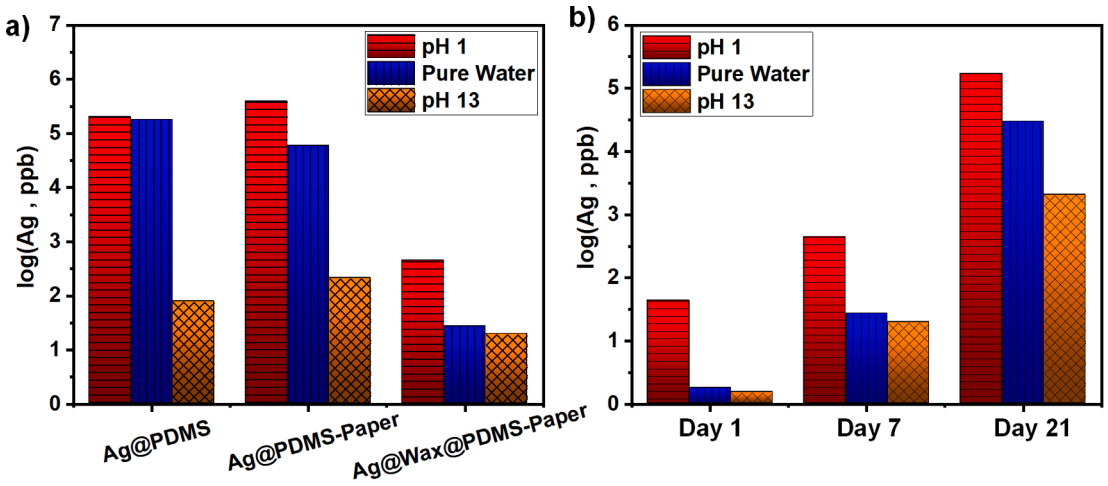

Fig. 6. Leaching test. a) Amount of leached Ag (log ppb) from the superhydrophobic Ag@Wax@PDMS-Paper surface in solutions with pH = 1, 7, and 13 after seven days. b) Amount of Ag leached from the superhydrophobic Ag@Wax@PDMS-Paper surface immersed in solutions with pH = 1, 7, and 13 after one day, 7 days, and 21 days.

probable that *E. coli* will attach to it [58,59]. For S. aureus (Fig. 3b, top row), there is no clear trend between surface hydrophobicity and the number of attached bacteria. It should be noted that S. aureus seems to also grow vertically and on top of each other. It is probably due to the increased colony-forming ability, small size, and spherical shape of S. aureus [4,59,60].

After the deposition of Ag, the number of attached *E. coli* and *S. aureus* are drastically reduced. Since coating with Ag does not seem to impact the wetting property of the surfaces (refer to Fig. 2c), it can be inferred that the increased anti-adhesion ability of the surfaces is due to the presence of Ag. The main reason for the reduced adhesion of bacteria could be due to small contact points between the bacteria and the Ag deposited surface due to increased nanoscale roughness [61]. It is also possible that bacteria killed by Ag do not strongly adhere to the sample surfaces. Furthermore, after being coated with Ag, there are more *E. coli* bacteria attached to the more hydrophobic (CA = 142°) Ag@PDMS-Paper surface than to the less hydrophobic (CA = 113°) Ag@PDMS surface. A careful examination reveals that colonies of *E. coli* are predominantly formed at the bottom, along the microchannels. This observation is similar to previous studies [62,63].

Shown in Fig. 4 are the results of the bactericidal test. First, the deposition of Ag makes all surfaces bactericidal to some degree. For *E. coli* transferred from Ag coated surfaces, only a handful of colonies are visibly grown on the agar plate, whereas the *E. coli* transferred from uncoated surfaces form dense colonies (Fig. 4a). For the S. aureus, there are a few dozen colonies grown even for bacteria transferred from Ag coated surfaces. However, the numbers are still very low compared to the grown S. aureus bacteria transferred from the uncoated surfaces (Fig. 4b). The UV–Vis absorbance values of bacterium suspension-cultured in the presence of various surfaces provides a quantitative value of bactericidal activity (also see supporting Fig. S11). As can be seen from Fig. 4c and 4d, all Ag coated surfaces achieve ~ 80 % bactericidal efficacy when compared to the uncoated corresponding surface, against both *E. coli* and S. aureus. The number of colonies is large on the Ag@PDMS-Paper surface for the *E. coli* (Fig. 4a). This observation is consistent with the anti-adhesion test results and indicates that *E. coli* can attach at the bottom along the microchannels and proliferate due to reduced deposition of Ag there. The antibacterial activity of various surfaces indicates that there are at least two mechanisms at play: i) contact killing where the surface structures induce deformation or even rapture of bacterial cell walls, leading to stress and death of bacteria. ii) killing via released Ag^{+} ions [64]. The second mechanism is possible since aqueous solutions (as in bacterial culture) cause oxidation of metallic Ag, which will subsequently dissolve. The possibility of Ag leaching raises questions about the long-term bactericidal activity of the superhydrophobic surface. The results of the bactericidal test (supporting Fig. S12) conducted on a superhydrophobic surface after being submerged in water for 7 days indicate a slight deterioration of bactericidal activity against *E. Coli*. However, the bactericidal activity against the more potent S. aureus was significantly reduced.

One application area of the SERS active and antibacterial superhydrophobic surface reported in this study is in food packaging where the antibacterial property enables extending shelf life and thus reduces food waste while the SERS activity can be utilized to detect harmful chemicals (such as rhodamine B in sausage) or other molecules of interest. Furthermore, the multifunctional surface also exhibits self-cleaning ability where water as well other liquid edibles like honey and pomegranate syrup easily roll off (supporting Fig. S13). It should be noted that the self-cleaning ability is beneficial for easy emptying of the content and reducing food waste in food processing facilities and packaging [65]. One of the main reasons for household food waste is due to the difficulty of emptying content where residual food, especially liquids with high viscosity, stuck to the packaging material surface and thrown away with the container [66]. To better characterize this, we measured surface tension of various liquids and their CA (supporting Table S1) on the multifunctional superhydrophobic surface (Fig. 5a). Furthermore, the amount of residual liquid stuck on various surfaces was also measured (Fig. 5b). For this purpose, we choose three sticky foods: Honey, yogurt, and pomegranate syrup. As shown in Fig. 5b, the amount of residual liquid stuck in conventional packaging materials like glass, aluminum, and PET is>20 % for all liquids while it is at most 3% for the superhydrophobic surface. Even larger contrast emerges when the test liquid food is pomegranate syrup: for glass, aluminum, and PET, the residual pomegranate syrup is close to 90 % whereas for our superhydrophobic surface, it is only 1.5 %. Therefore, the fabricated superhydrophobic surface represents a highly promsing packaging material when considering mitigating residual food waste.

An important factor when considering materials for food packaging is safety: the packaging material should not release toxic chemicals into the food that it comes in contact with [45]. Since the main components of the superhydrophobic Ag@Wax@PDMS-Paper surface are PDMS and carnauba wax (Ag is only ~ 2%, see supporting Fig. S3) both of which are ecofriendly and biocompatible [47,53]. Notwithstanding, the minor component Ag may raise concerns due to reported toxicity [45,67]. Therefore, we performed a leaching test by immersing the superhydrophobic surface in solutions with pH values of 1 and 13, and in pure water (Fig. 6), followed by measuring leached Ag concentration using

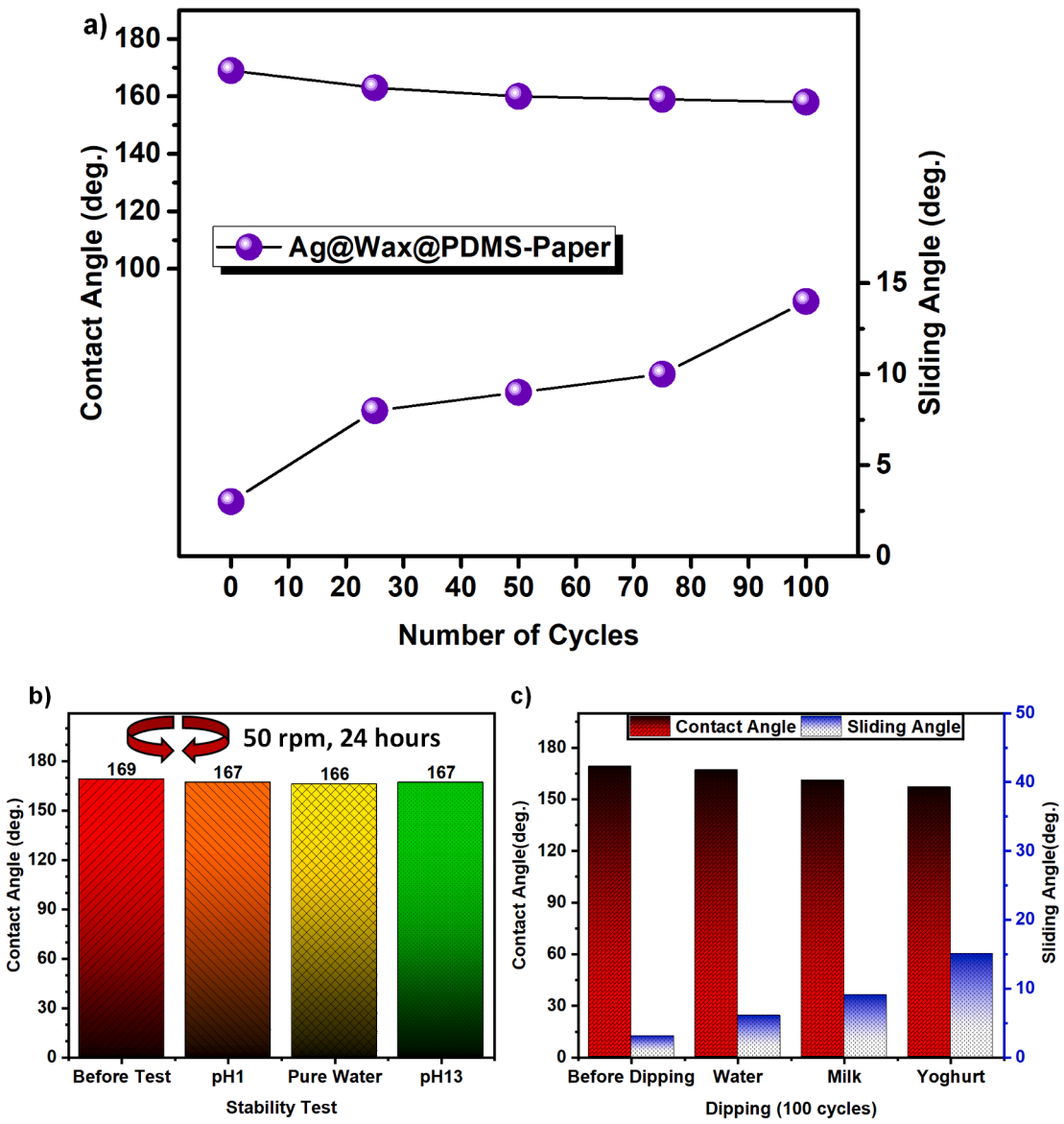

Fig. 7. Results of various durability tests performed on the superhydrophobic surface. a) water spray impact test. b) stability test underwater under mechanical stirring. c) water CA and SA values on the superhydrophobic surface measured after 100 cycles of immersion into various liquids.

ICP-MS. It should be noted that the nominal pH value of foods is between 3 (orange juice) and 8 (shrimp). Thus, our leaching condition simulates much harsher conditions than those that could be encountered in real-world samples.

As can be seen from Fig. 6a, the amount of leached Ag from the superhydrophobic surface in all solutions is approximately three orders of magnitude lower than the other two control surfaces (Ag@PDMS and Ag@PDMS-Paper). The reduced leaching from the superhydrophobic surface is probably due to the small contact area of the liquid, which occurs on the asperities of the rough texture [68,69]. However, we could not rule out the possible complexation between Ag and carnauba wax molecules, which can also reduce leaching. Another clear trend in Fig. 6a is that the amount of leached Ag is higher in solutions with lower pH values. For example, the amount of leached Ag from the superhydrophobic surface immersed in a solution with pH = 1 is 438 ppb, which is 16 times that of solution with pH = 7 (water) and 22 times that of solution with pH = 13 (See supporting Table S2 for exact values). The trend of increased leaching of Ag at a lower pH is consistent with previous studies [64,67,68]. A long-term (up to 21 days) test revealed that more Ag is leached into the solution as the days of immersion increased (Fig. 6b). After being immersed in acidic (pH = 1), neutral (pH = 7), and basic (pH = 13) solutions for 7 days, the amount of leached Ag is 453.10 ppb, 26.86 ppb, and 19.50 ppb, respectively (supporting Table S2). The maximum leaching occurred in acidic conditions is above the safety limit but in the neutral and basic conditions, the leached amount of Ag is within the acceptable limit (50 ppb) set by European regulations required for materials that contact food [70]. Therefore, the superhydrophobic Ag@Wax@PDMS-Paper can be considered safe in food packaging applications, at least within a short storage time (7 days).

Limited durability of the superhydrophobic surfaces is one of the main reasons impeding their practical application. To evaluate the real-life application potential of the superhydrophobic surface, we performed several durability tests. The surface retained its superhydrophobicity up to 78 °C of annealing (supporting Fig. S14), similar to previous superhydrophobic surfaces fabricated from carnauba wax [41,53,71]. This indicates that the addition of a small amount of Ag does not affect the thermal stability of the superhydrophobic surface. The durability of the superhydrophobic surface under various dynamic conditions is shown in Fig. 7 below. The surface can withstand 100 cycles of water spray impact under the impact pressure of 7.41 kPa.

Elemental analysis of the sample surface before and after water spray impact shows only a slight decrease of Ag (supporting Fig. S15), indicating a relatively strong bonding of Ag to the surface. Even though the water CA is still above 150° after the impact, the SA increased to above 10° (Fig. 7a). This loss of superhydrophobicity is probably due to the transition from Cassie-Baxter state to Wenzel state where the movement of liquid droplets is hindered. Under dynamic conditions, the superhydrophobic surface showed at least 24 h stability underwater which was kept stirred at 50 rpm (Fig. 7b). An important and harsh test, especially concerning food packaging is the immersion test [72–74]. This test simulates the durability of a surface against relative movement of a liquid, which occurs when filling or emptying the content of packaged food, or during transportation. The immersion test was performed against three different liquids, water, milk, and yogurt (Fig. 7c). The surface retains its superhydrophobicity even after 100 cycles of immersion in water and milk. The performance is very good concerning milk, which is a mixture of complex molecules and proteins (~6%). The surface loses its superhydrophobicity after 100 cycles of immersion into yogurt, which contains up to 20 % of various proteins. Notwithstanding, the performance against yogurt is better or on par with previous studies [73,74]. The reduced anti-fouling ability of the superhydrophobic surface under dynamic conditions against liquids that contain protein may be due to the strong bonding of some thiol functional groups (as in cysteine) to Ag.

4. Conclusion

A multi-functional superhydrophobic surface is fabricated from ecofriendly and biocompatible materials. The physical vapor deposition of Ag imparted SERS and antibacterial activity to the superhydrophobic Wax@PDMS-Paper surface. The SERS activity and liquid repellency are found to depend on the thickness of the Ag film. Furthermore, we demonstrated that this SERS active superhydrophobic surface can be used to detect adulterant rhodamine B in sausages down to nM levels. Furthermore, the adhesion of both *E. coli* and *S. aureus* bacteria was significantly reduced due to superhydrophobicity. Besides the bacterial anti-adhesion ability, the Ag coated superhydrophobic Ag@Wax@PDMS-Paper surface showed excellent antibacterial activity against two of the most common antimicrobial-resistant bacteria, *E. coli* and *S. aureus* with the efficacy of 99.37 % and 93.48 %, respectively.

In addition to the SERS and antibacterial activity, the fabricated superhydrophobic surface also showed self-cleaning properties against common liquid food. Here, even the sticky liquid foods can easily roll off from the superhydrophobic surface, leaving behind at most 2 % residual food. Notably, the superhydrophobic surface showed good chemical stability and leaching of Ag from the superhydrophobic surface is minimal. Furthermore, the superhydrophobic surface showed good thermal and mechanical stability under realistic conditions. Therefore, the antifouling, SERS active, and the antibacterial superhydrophobic surfaces are a step closer to bring superhydrophobic coatings and surfaces to real-life applications where extra functionalities besides mere water repellency are desired.

Declaration of Competing Interest

The authors declare that they have no known competing financial interests or personal relationships that could have appeared to influence the work reported in this paper.

Acknowledgment

This work was supported by the Research Fund of the Erciyes University (project number FDK-2021-11321). This work constitutes part of the doctoral thesis of FS who acknowledges the financial support from the Council of Higher Education of Turkey (100/2000 YÖK Doctoral Scholarship). MSO acknowledges partial support from The Science Academy, Turkey through the Young Scientist Award Program.

Appendix A. Supplementary data

Supplementary data to this article can be found online at https://doi.org/10.1016/j.cej.2021.133445.

References

[1] M.E.A. de Kraker, P.G. Davey, H. Grundmann, S.M. Opal, Mortality and Hospital Stay Associated with Resistant Staphylococcus aureus and Escherichia coli Bacteremia: Estimating the Burden of Antibiotic Resistance in Europe, PLoS Med. 8 (10) (2011) e1001104, https://doi.org/10.1371/journal.pmed.1001104.

[2] J.M. Boyce, Environmental contamination makes an important contribution to hospital infection, J. Hosp. Infect. 65 (2007) 50–54, https://doi.org/10.1016/S0195-6701(07)60015-2.

[3] W. DeFlorio, S. Liu, A.R. White, T.M. Taylor, L. Cisneros-Zevallos, Y. Min, E.M. A. Scholar, Recent developments in antimicrobial and antifouling coatings to reduce or prevent contamination and cross-contamination of food contact surfaces by bacteria, Compr. Rev. Food Sci. Food Saf. 20 (2021) 3093–3134, https://doi.org/10.1111/1541-4337.12750.

[4] J.K. Oh, Y. Yegin, F. Yang, M. Zhang, J. Li, S. Huang, S.V. Verkhoturov, E. A. Schweikert, K. Perez-Lewis, E.A. Scholar, T.M. Taylor, A. Castillo, L. Cisneros-Zevallos, Y. Min, M. Akbulut, The influence of surface chemistry on the kinetics and thermodynamics of bacterial adhesion, Sci. Rep. 8 (2018) 17247, https://doi.org/10.1038/s41598-018-35343-1.

[5] B. Song, E. Zhang, X. Han, H. Zhu, Y. Shi, Z. Cao, Engineering and Application Perspectives on Designing an Antimicrobial Surface, ACS Appl. Mater. Interfaces. 12 (19) (2020) 21330–21341, https://doi.org/10.1021/acsami.9b19992.

[6] T.J. Hall, V.M. Villapún, O. Addison, M.A. Webber, M. Lowther, S.E.T. Louth, S. E. Mountcastle, M.Y. Brunet, S.C. Cox, A call for action to the biomaterial community to tackle antimicrobial resistance, Biomater. Sci. 8 (18) (2020) 4951–4974, https://doi.org/10.1039/D0BM01160F.

[7] F. Hizal, N. Rungraeng, J. Lee, S. Jun, H.J. Busscher, H.C. van der Mei, C.-H. Choi, Nanoengineered Superhydrophobic Surfaces of Aluminum with Extremely Low Bacterial Adhesivity, ACS Appl. Mater. Interfaces. 9 (13) (2017) 12118–12129, https://doi.org/10.1021/acsami.7b0132210.1021/acsami.7b01322.s001.

[8] H.R. Hong, J. Kim, C.H. Park, Facile fabrication of multifunctional fabrics: use of copper and silver nanoparticles for antibacterial, superhydrophobic, conductive fabrics, RSC Adv. 8 (73) (2018) 41782–41794, https://doi.org/10.1039/C8RA08310J.

[9] T. Ren, M. Yang, K. Wang, Y. Zhang, J. He, CuO Nanoparticles-Containing Highly Transparent and Superhydrophobic Coatings with Extremely Low Bacterial Adhesion and Excellent Bactericidal Property, ACS Appl. Mater. Interfaces. 10 (30) (2018) 25717–25725, https://doi.org/10.1021/acsami.8b0994510.1021/acsami.8b09945.s001.

[10] E. Ozkan, A. Mondal, P. Singha, M. Douglass, S.P. Hopkins, R. Devine, M. Garren, J. Manuel, J. Warnock, H. Handa, Fabrication of Bacteria- and Blood-Repellent Superhydrophobic Polyurethane Sponge Materials, ACS Appl. Mater. Interfaces. 12 (46) (2020) 51160–51173, https://doi.org/10.1021/acsami.0c13098.

[11] A.B.D. Cassie, S. Baxter, Wettability of porous surfaces, Trans. Faraday Soc. 40 (1944) 546–551, https://doi.org/10.1039/TF9444000546.

[12] A. Lafuma, D. Quéré, Superhydrophobic states, Nat. Mater. 2 (7) (2003) 457–460, https://doi.org/10.1038/nmat924.

[13] X.-F. Zhang, Y.-Q. Chen, J.-M. Hu, Robust superhydrophobic SiO2/polydimethylsiloxane films coated on mild steel for corrosion protection, Corros. Sci. 166 (2020) 108452, https://doi.org/10.1016/j.corsci.2020.108452.

[14] X. Yin, S. Yu, K. Wang, R. Cheng, Z. Lv, Fluorine-free preparation of self-healing and anti-fouling superhydrophobic Ni3S2 coating on 304 stainless steel, Chem. Eng. J. 394 (2020) 124925, https://doi.org/10.1016/j.cej.2020.124925.

[15] N. Celik, S. Altındal, Z. Gozutok, M. Ruzi, M.S. Onses, Effect of fabric texture on the durability of fluorine-free superhydrophobic coatings, J. Coatings Technol. Res. 17 (3) (2020) 785–796, https://doi.org/10.1007/s11998-020-00333-4.

[16] Z. She, Q. Li, Z. Wang, L. Li, F. Chen, J. Zhou, Researching the fabrication of anticorrosion superhydrophobic surface on magnesium alloy and its mechanical stability and durability, Chem. Eng. J. 228 (2013) 415–424, https://doi.org/10.1016/j.cej.2013.05.017.

[17] D. Zang, R. Zhu, W. Zhang, X. Yu, L. Lin, X. Guo, M. Liu, L. Jiang, Corrosion-Resistant Superhydrophobic Coatings on Mg Alloy Surfaces Inspired by Lotus Seedpod, Adv. Funct. Mater. 27 (8) (2017) 1605446, https://doi.org/10.1002/adfm.v27.810.1002/adfm.201605446.

[18] G.B. Hwang, K. Page, A. Patir, S.P. Nair, E. Allan, I.P. Parkin, The Anti-Biofouling Properties of Superhydrophobic Surfaces are Short-Lived, ACS Nano. 12 (6) (2018) 6050–6058, https://doi.org/10.1021/acsnano.8b0229310.1021/acsnano.8b02293.s00110.1021/acsnano.8b02293.s002.

[19] S.M.R. Razavi, J. Oh, R.T. Haasch, K. Kim, M. Masoomi, R. Bagheri, J.M. Slauch, N. Miljkovic, Environment-Friendly Antibiofouling Superhydrophobic Coatings, ACS Sustain. Chem. Eng. 7 (17) (2019) 14509–14520, https://doi.org/10.1021/acssuschemeng.9b02025.

[20] S. Naderizadeh, S. Dante, P. Picone, M. Di Carlo, R. Carzino, A. Athanassiou, I. S. Bayer, Bioresin-based superhydrophobic coatings with reduced bacterial adhesion, J. Colloid Interface Sci. 574 (2020) 20–32, https://doi.org/10.1016/j.jcis.2020.04.031.

[21] Y. Wang, X. Liu, H. Zhang, Z. Zhou, Superhydrophobic surfaces created by a one-step solution-immersion process and their drag-reduction effect on water, RSC Adv. 5 (24) (2015) 18909–18914, https://doi.org/10.1039/C5RA00941C.

[22] M. Rezaei, P. Radfar, M. Winter, L. McClements, B. Thierry, M.E. Warkiani, Simple-to-Operate Approach for Single Cell Analysis Using a Hydrophobic Surface and Nanosized Droplets, Anal. Chem. 93 (10) (2021) 4584–4592, https://doi.org/10.1021/acs.analchem.0c0502610.1021/acs.analchem.0c05026.s001.

[23] K. Ellinas, D. Kefallinou, K. Stamatakis, E. Gogolides, A. Tserepi, Is There a Threshold in the Antibacterial Action of Superhydrophobic Surfaces? ACS Appl. Mater. Interfaces. 9 (45) (2017) 39781–39789, https://doi.org/10.1021/acsami.7b11402.

[24] N. Encinas, C.-Y. Yang, F. Geyer, A. Kaltbeitzel, P. Baumli, J. Reinholz, V. Mailänder, H.-J. Butt, D. Vollmer, Submicrometer-Sized Roughness Suppresses Bacteria Adhesion, ACS Appl. Mater. Interfaces. 12 (19) (2020) 21192–21200, https://doi.org/10.1021/acsami.9b22621.

[25] R.N. Wenzel, Resistance of solid surfaces to wetting by water, Ind. Eng. Chem. 28 (8) (1936) 988–994, https://doi.org/10.1021/ie50320a024.

[26] F. Geyer, M. D'Acunzi, A. Sharifi-Aghili, A. Saal, N. Gao, A. Kaltbeitzel, T.F. Sloot, R. Berger, H.J. Butt, D. Vollmer, When and how self-cleaning of superhydrophobic surfaces works, Sci. Adv. 6 (2020) eaaw9727, https://doi.org/10.1126/sciadv.aaw9727.

[27] C. Marambio-Jones, E.M.V. Hoek, A review of the antibacterial effects of silver nanomaterials and potential implications for human health and the environment, J. Nanoparticle Res. 12 (5) (2010) 1531–1551, https://doi.org/10.1007/s11051-010-9900-y.

[28] P. Qi, Z. Lin, J. Li, C. Wang, W. Meng, H. Hong, X. Zhang, Development of a rapid, simple and sensitive HPLC-FLD method for determination of rhodamine B in chili-containing products, Food Chem. 164 (2014) 98–103, https://doi.org/10.1016/j.foodchem.2014.05.036.

[29] A. Tripathy, S. Sreedharan, C. Bhaskarla, S. Majumdar, S.K. Peneti, D. Nandi, P. Sen, Enhancing the Bactericidal Efficacy of Nanostructured Multifunctional Surface Using an Ultrathin Metal Coating, Langmuir. 33 (44) (2017) 12569–12579, https://doi.org/10.1021/acs.langmuir.7b02291.

[30] F. De Angelis, F. Gentile, F. Mecarini, G. Das, M. Moretti, P. Candeloro, M. L. Coluccio, G. Cojoc, A. Accardo, C. Liberale, R.P. Zaccaria, G. Perozziello, L. Tirinato, A. Toma, G. Cuda, R. Cingolani, E. Di Fabrizio, Breaking the diffusion limit with super-hydrophobic delivery of molecules to plasmonic nanofocusing SERS structures, Nat. Photonics. 5 (11) (2011) 682–687, https://doi.org/10.1038/nphoton.2011.222.

[31] J. Langer, D. Jimenez de Aberasturi, J. Aizpurua, R.A. Alvarez-Puebla, B. Auguié, J. J. Baumberg, G.C. Bazan, S.E.J. Bell, A. Boisen, A.G. Brolo, J. Choo, D. Cialla-May, V. Deckert, L. Fabris, K. Faulds, F.J. García de Abajo, R. Goodacre, D. Graham, A. J. Haes, C.L. Haynes, C. Huck, T. Itoh, M. Käll, J. Kneipp, N.A. Kotov, H. Kuang, E. C. Le Ru, H.K. Lee, J.-F. Li, X.Y. Ling, S.A. Maier, T. Mayerhöfer, M. Moskovits, K. Murakoshi, J.-M. Nam, S. Nie, Y. Ozaki, I. Pastoriza-Santos, J. Perez-Juste, J. Popp, A. Pucci, S. Reich, B. Ren, G.C. Schatz, T. Shegai, S. Schlücker, L.-L. Tay, K. G. Thomas, Z.-Q. Tian, R.P. Van Duyne, T. Vo-Dinh, Y. Wang, K.A. Willets, C. Xu, H. Xu, Y. Xu, Y.S. Yamamoto, B. Zhao, L.M. Liz-Marzán, Present and Future of Surface-Enhanced Raman Scattering, ACS Nano. 14 (1) (2020) 28–117, https://doi.org/10.1021/acsnano.9b04224.

[32] X. Wang, N. Li, D. Xu, X. Yang, Q. Zhu, D. Xiao, N. Lu, Superhydrophobic candle soot/PDMS substrate for one-step enrichment and desalting of peptides in MALDI MS analysis, Talanta. 190 (2018) 23–29, https://doi.org/10.1016/j.talanta.2018.07.066.

[33] J.K. Oh, S. Liu, M. Jones, Y. Yegin, L. Hao, T.N. Tolen, N. Nagabandi, E.A. Scholar, A. Castillo, T.M. Taylor, L. Cisneros-Zevallos, M. Akbulut, Modification of aluminum surfaces with superhydrophobic nanotextures for enhanced food safety and hygiene, Food Control. 96 (2019) 463–469, https://doi.org/10.1016/j.foodcont.2018.10.005.

[34] V. Moreno, K. Murtada, M. Zougagh, Á. Ríos, Analytical control of Rhodamine B by SERS using reduced graphene decorated with copper selenide, Spectrochim, Acta Part A Mol. Biomol. Spectrosc. 223 (2019) 117302, https://doi.org/10.1016/j.saa.2019.117302.

[35] Y. Sun, W. Li, L. Zhao, F. Li, Y. Xie, W. Yao, W. Liu, Z. Lin, Simultaneous SERS detection of illegal food additives rhodamine B and basic orange II based on Au nanorod-incorporated melamine foam, Food Chem. 357 (2021) 129741, https://doi.org/10.1016/j.foodchem.2021.129741.

[36] J. Li, J. Tian, Y. Gao, R. Qin, H. Pi, M. Li, P. Yang, All-natural superhydrophobic coating for packaging and blood-repelling materials, Chem. Eng. J. 410 (2021) 128347, https://doi.org/10.1016/j.cej.2020.128347.

[37] D. Wang, J. Huang, Z. Guo, Tomato-lotus inspired edible superhydrophobic artificial lotus leaf, Chem. Eng. J. 400 (2020) 125883, https://doi.org/10.1016/j.cej.2020.125883.

[38] W. Wang, K. Lockwood, L.M. Boyd, M.D. Davidson, S. Movafaghi, H. Vahabi, S. R. Khetani, A.K. Kota, Superhydrophobic Coatings with Edible Materials, ACS Appl. Mater. Interfaces. 8 (29) (2016) 18664–18668, https://doi.org/10.1021/acsami.6b06958.

[39] Y. Li, J. Bi, S. Wang, T. Zhang, X. Xu, H. Wang, S. Cheng, B.-W. Zhu, M. Tan, Bio-inspired Edible Superhydrophobic Interface for Reducing Residual Liquid Food, J. Agric. Food Chem. 66 (9) (2018) 2143–2150, https://doi.org/10.1021/acs.jafc.7b05915.

[40] X. Zhao, T. Hu, J. Zhang, Superhydrophobic coatings with high repellency to daily consumed liquid foods based on food grade waxes, J. Colloid Interface Sci. 515 (2018) 255–263, https://doi.org/10.1016/j.jcis.2018.01.034.

[41] Y. Zhang, J. Bi, S. Wang, Q. Cao, Y. Li, J. Zhou, B.-W. Zhu, Functional food packaging for reducing residual liquid food: Thermo-resistant edible super-hydrophobic coating from coffee and beeswax, J. Colloid Interface Sci. 533 (2019) 742–749, https://doi.org/10.1016/j.jcis.2018.09.011.

[42] H. Forbes, T. Quested, C. O'Connor, UNEP Food Waste Index Report 2021 | UNEP - UN Environment Programme, 2021. https://www.unep.org/resources/report/unep-food-waste-index-report-2021 (accessed June 9, 2021).

[43] I.S. Bayer, Superhydrophobic Coatings from Ecofriendly Materials and Processes: A Review, Adv. Mater. Interfaces. 7 (13) (2020) 2000095, https://doi.org/10.1002/admi.v7.1310.1002/admi.202000095.

[44] N. Celik, I. Torun, M. Ruzi, A. Esidir, M.S. Onses, Fabrication of robust superhydrophobic surfaces by one-step spray coating: Evaporation driven self-assembly of wax and nanoparticles into hierarchical structures, Chem. Eng. J. 396 (2020) 125230, https://doi.org/10.1016/j.cej.2020.125230.

[45] S. Chernousova, M. Epple, Silver as Antibacterial Agent: Ion, Nanoparticle, and Metal, Angew. Chemie Int. Ed. 52 (6) (2013) 1636–1653, https://doi.org/10.1002/anie.v52.610.1002/anie.201205923.

[46] N. Celik, I. Torun, M. Ruzi, M.S. Onses, Robust superhydrophobic fabrics by infusing structured polydimethylsiloxane films, J. Appl. Polym. Sci. 138 (41) (2021) 51358, https://doi.org/10.1002/app.51358.

[47] I. Torun, N. Celik, M. Ruzi, M.S. Onses, Transferring the structure of paper for mechanically durable superhydrophobic surfaces, Surf. Coatings Technol. 405 (2021) 126543, https://doi.org/10.1016/j.surfcoat.2020.126543.

[48] V.L. Schlegel, T.M. Cotton, Silver-island films as substrates for enhanced Raman scattering: effect of deposition rate on intensity, Anal. Chem. 63 (3) (1991) 241–247, https://doi.org/10.1021/ac00003a010.

[49] F. Foadi, S.M. Vaez Allaei, G. Palasantzas, M.R. Mohammadizadeh, Roughness-dependent wetting behavior of vapor-deposited metallic thin films, Phys. Rev. E. 100 (2019), 022804, https://doi.org/10.1103/PhysRevE.100.022804.

[50] S. Lin, W.-L.-J. Hasi, X. Lin, S.-Q.-G.-w. Han, X.-T. Lou, F. Yang, D.-Y. Lin, Z.-W. Lu, Rapid and sensitive SERS method for determination of Rhodamine B in chili powder with paper-based substrates, Anal. Methods. 7 (12) (2015) 5289–5294, https://doi.org/10.1039/C5AY00028A.

[51] J. Haldar, A.K. Weight, A.M. Klibanov, Preparation, application and testing of permanent antibacterial and antiviral coatings, Nat. Protoc. 2 (10) (2007) 2412–2417, https://doi.org/10.1038/nprot.2007.353.

[52] X. Liu, L. Wang, Y. Qiao, X. Sun, S. Ma, X. Cheng, W. Qi, W. Huang, Y. Li, Adhesion of liquid food to packaging surfaces: Mechanisms, test methods, influencing factors and anti-adhesion methods, J. Food Eng. 228 (2018) 102–117, https://doi.org/10.1016/j.jfoodeng.2018.02.002.

[53] N. Celik, F. Sahin, M. Ruzi, M. Yay, E. Unal, M.S. Onses, Blood repellent superhydrophobic surfaces constructed from nanoparticle-free and biocompatible materials, Colloids Surfaces B Biointerfaces. 205 (2021) 111864, https://doi.org/10.1016/j.colsurfb.2021.111864.

[54] X. Liang, H. Zhang, C. Xu, D. Cao, Q. Gao, S.i. Cheng, Condensation effect-induced improved sensitivity for SERS trace detection on a superhydrophobic plasmonic nanofibrous mat, RSC Adv. 7 (70) (2017) 44492–44498, https://doi.org/10.1039/C7RA09194J.

[55] M.J. Natan, Concluding Remarks : Surface enhanced Raman scattering, Faraday Discuss. 132 (2006) 321, https://doi.org/10.1039/b601494c.

[56] F. Liang, D. Jin, P. Ma, D.i. Wang, Q. Yang, D. Song, X. Wang, Rapid Determination of Rhodamine B in Chili Powder by Surface-Enhanced Raman Spectroscopy, Anal. Lett. 48 (12) (2015) 1918–1929, https://doi.org/10.1080/00032719.2014.1003428.

[57] X. Zhang, L. Wang, E. Levänen, Superhydrophobic surfaces for the reduction of bacterial adhesion, RSC Adv. 3 (30) (2013) 12003, https://doi.org/10.1039/c3ra40497h.

[58] C.R. Crick, S. Ismail, J. Pratten, I.P. Parkin, An investigation into bacterial attachment to an elastomeric superhydrophobic surface prepared via aerosol assisted deposition, Thin Solid Films. 519 (11) (2011) 3722–3727, https://doi.org/10.1016/j.tsf.2011.01.282.

[59] K. Schwibbert, F. Menzel, N. Epperlein, J. Bonse, J. Krüger, Bacterial Adhesion on Femtosecond Laser-Modified Polyethylene, Materials (Basel). 12 (19) (2019) 3107, https://doi.org/10.3390/ma12193107.

[60] W.K. Jung, H.C. Koo, K.W. Kim, S. Shin, S.H. Kim, Y.H. Park, Antibacterial Activity and Mechanism of Action of the Silver Ion in Staphylococcus aureus and Escherichia coli, Appl. Environ. Microbiol. 74 (7) (2008) 2171–2178, https://doi.org/10.1128/AEM.02001-07.

[61] C. Dewald, C. Lüdecke, I. Firkowska-Boden, M. Roth, J. Bossert, K.D. Jandt, Gold nanoparticle contact point density controls microbial adhesion on gold surfaces, Colloids Surfaces B Biointerfaces. 163 (2018) 201–208, https://doi.org/10.1016/j.colsurfb.2017.12.037.

[62] H. Gu, A. Chen, X. Song, M.E. Brasch, J.H. Henderson, D. Ren, How Escherichia coli lands and forms cell clusters on a surface: a new role of surface topography, Sci. Rep. 6 (2016) 29516, https://doi.org/10.1038/srep29516.

[63] D. Perera-Costa, J.M. Bruque, M.L. González-Martín, A.C. Gómez-García, V. Vadillo-Rodríguez, Studying the Influence of Surface Topography on Bacterial Adhesion using Spatially Organized Microtopographic Surface Patterns, Langmuir. 30 (16) (2014) 4633–4641, https://doi.org/10.1021/la5001057.

[64] Z.-M. Xiu, Q.-b. Zhang, H.L. Puppala, V.L. Colvin, P.J.J. Alvarez, Negligible Particle-Specific Antibacterial Activity of Silver Nanoparticles, Nano Lett. 12 (8) (2012) 4271–4275, https://doi.org/10.1021/nl301934w.

[65] M. Wang, Y. Zi, J. Zhu, W. Huang, Z. Zhang, H. Zhang, Construction of super-hydrophobic PDMS@MOF@Cu mesh for reduced drag, anti-fouling and self-cleaning towards marine vehicle applications, Chem. Eng. J. 417 (2021) 129265, https://doi.org/10.1016/j.cej.2021.129265.

[66] H. Williams, F. Wikström, T. Otterbring, M. Löfgren, A. Gustafsson, Reasons for household food waste with special attention to packaging, J. Clean. Prod. 24 (2012) 141–148, https://doi.org/10.1016/j.jclepro.2011.11.044.
[67] T. Yang, T. Paulose, B.W. Redan, J.C. Mabon, T.V. Duncan, Food and Beverage Ingredients Induce the Formation of Silver Nanoparticles in Products Stored within Nanotechnology-Enabled Packaging, ACS Appl. Mater. Interfaces. 13 (1) (2021) 1398–1412, https://doi.org/10.1021/acsami.0c1786710.1021/acsami.0c17867.s001.
[68] S. Heinonen, E. Huttunen-Saarivirta, J.-P. Nikkanen, M. Raulio, O. Priha, J. Laakso, E. Storgårds, E. Levänen, Antibacterial properties and chemical stability of superhydrophobic silver-containing surface produced by sol–gel route, Colloids Surfaces A Physicochem. Eng. Asp. 453 (2014) 149–161, https://doi.org/10.1016/j.colsurfa.2014.04.037.
[69] L. Zhang, L. Zhang, Y. Yang, W. Zhang, H. Lv, F. Yang, C. Lin, P. Tang, Inhibitory effect of super-hydrophobicity on silver release and antibacterial properties of super-hydrophobic Ag/TiO 2 nanotubes, J. Biomed. Mater. Res. Part B Appl. Biomater. 104 (5) (2016) 1004–1012, https://doi.org/10.1002/jbm.b.v104.510.1002/jbm.b.33454.
[70] N. von Goetz, L. Fabricius, R. Glaus, V. Weitbrecht, D. Günther, K. Hungerbühler, Migration of silver from commercial plastic food containers and implications for consumer exposure assessment, Food Addit, Contam. - Part A Chem. Anal. Control. Expo. Risk Assess. 30 (3) (2013) 612–620, https://doi.org/10.1080/19440049.2012.762693.
[71] N. Celik, N.B. Kiremitler, M. Ruzi, M.S. Onses, Waxing the soot: Practical fabrication of all-organic superhydrophobic coatings from candle soot and carnauba wax, Prog. Org. Coatings. 153 (2021) 106169, https://doi.org/10.1016/j.porgcoat.2021.106169.
[72] J.A. Barish, J.M. Goddard, Anti-fouling surface modified stainless steel for food processing, Food Bioprod. Process. 91 (4) (2013) 352–361, https://doi.org/10.1016/j.fbp.2013.01.003.
[73] T. Shen, S. Fan, Y. Li, G. Xu, W. Fan, Preparation of edible non-wettable coating with soybean wax for repelling liquid foods with little residue, Materials (Basel). 13 (2020) 3308, https://doi.org/10.3390/ma13153308.
[74] B.Y. Liu, C.H. Xue, Q.F. An, S.T. Jia, M.M. Xu, Fabrication of superhydrophobic coatings with edible materials for super-repelling non-Newtonian liquid foods, Chem. Eng. J. 371 (2019) 833–841, https://doi.org/10.1016/j.cej.2019.03.222.